

ACCURATE ANALYSIS OF SHALLOW SOLAR WIND ION IMPLANTS BY SIMS BACKSIDE DEPTH PROFILING. V.S. Heber¹, K.D. McKeegan¹, S. Smith², A.J.G. Jurewicz³, C. Olinger⁴, D.S. Burnett⁵, Y. Guan⁵; 1 Dept. Earth, Planetary, and Space Sciences, UCLA, Los Angeles, CA, USA, heber@ess.ucla.edu; 2 Evans Analytical Group, Sunnyvale, CA, USA; 3 Arizona State University, Tempe, AZ, USA; 4 LANL, Neutron Science and Technology, Los Alamos, USA; 5 California Institute of Technology, Pasadena, CA, USA.

Introduction: The NASA mission “Genesis” collected solar wind (SW) for laboratory analysis [1]. SW can serve as a proxy for the Sun’s composition, and thus the average composition of the solar nebula [2], provided that fractionation processes during SW formation [e.g., 3] can be understood and quantitatively modeled. The Genesis objective is to obtain elemental and isotopic abundances with precisions and accuracies better than available spacecraft data, which have uncertainties of up to several tens of percent [4].

SW ions travel with an average speed of 400km/s, (~1keV/amu) at 1 AU; thus, SW is implanted with a mean depth of ~40nm into exposed collectors. The highest energy SW ions (up to 1200km/s) penetrate up to ~600nm deep. Despite the purity of the collector materials, contamination of their surfaces is significant: a natural oxide layer, a molecular film deposited in space [5], and particles deposited during the hard landing are all present.

Here, we present a technique that is capable of analyzing nearly complete depth distributions of many elements in the SW even in the presence of high levels of surface contamination: backside depth profiling by secondary ion mass spectrometry (SIMS), which we have successfully applied to the analysis of bulk SW with fluence as low as 2×10^{10} atoms/cm² and also of all three SW regimes for some more abundant elements. A low impact energy primary ion beam and oxygen flooding are used to minimize ion beam mixing of surface contamination and transient effects on SIMS ion yields. We discuss sample preparation, analytical conditions, standardization, and data reduction as well as potential systematic errors.

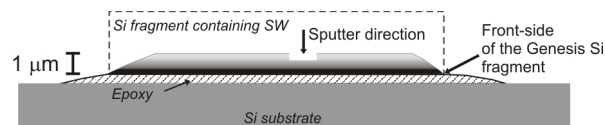


Fig. 1. Schematic edge-on view of a backside sample.

Backside depth profiling: The low concentration of the SW implant and its shallow depth require exceptional measures to obtain accurate depth profiles. Even with the high depth-resolution inherent in SIMS, knock-on of ions from a high-concentration region (surface contamination) to a low concentration region (SW) is problematic during conventional front-side SIMS depth profiling [7]. For backside depth profiling, cleaned Si fragments from the bulk and all three SW

regimes were ground to thicknesses between 0.5–1μm after attaching them, upside down, onto a Si substrate with epoxy (Fig. 1). The thickness of the sample was monitored during preparation to ± 100 nm by using spectral reflectometry. We have found that the optimum thickness of a backside SW sample is ~0.8μm, allowing sufficient space (~200 nm) between the surface contamination and the starting SW signal for background characterization [Fig. 3 in 8] and also a reasonable total analysis time.

SIMS analytical conditions: Analyses were performed with the Cameca 7f-Geo at Caltech and the Cameca IMS-1270 at UCLA. To date we have analyzed Na, Mg, Al, and Ca in all SW regimes, as well as C, N, O and Cr in bulk SW [9]. We used low impact energies for the primary ion beam (5keV for $^{133}\text{Cs}^+$ and 7.5keV for O_2^+) to increase the depth resolution. The primary beam was rastered over a $100\mu\text{m} \times 100\mu\text{m}$ area and the current adjusted to achieve a sputter rate (S) of 0.1–0.2nm/s (positive ions) and 0.24nm/s for C, N, O (negative ions). The primary beam was tuned to have a homogeneous density distribution to produce a flat break-through at the end of the analysis (which was monitored optically during the measurement). Secondary ions were selected from the center of the crater by using the field aperture. Mass resolving power was adjusted as needed for the element of interest. A $\sim 10^{-5}$ Torr O_2 bleed into the sample chamber was used to reduce initial non-equilibrium sputtering and increase secondary ion signals (positive ions).

Sample analysis: Each element was analyzed separately and SW analyses were bracketed by standard reference implants measured alternately in the same 7mm center-hole holder (except for C, N, O analysis where vacuum considerations excluded sample changes, a 4-hole Cameca holder was used). The primary beam current and Si (matrix element) countrates were constant within ~1% over few hours, an important condition as the depth of a backside profile was calculated from S of the adjacent standards. Instrumental background due to tertiary ion sputtering from the immersion lens was reduced by intense (150nA, 500μm raster) overnight Si sputtering to cover contamination. SW profiles were analyzed by stepwise sputtering: (1) a 125μm raster removed surface contamination, then a 100μm raster for analysis (steps 2–4). During steps (1) and (2) both the isotope of interest and Si were measured; during step (3) only the isotope of interest was

monitored to mitigate loss of SW data due to magnetic field peak jumping. Finally, in step (4), the Si countrate was checked on an adjacent spot. Artificial ion implants with known nominal fluences served as references from which relative sensitivity factors were obtained to calculate SW fluences. Crater pit depths were measured with an interferometer. For some elements (e.g., Mg) we were able to absolutely calibrate the reference implant fluence [10].

Measured – modeled SW depth profile comparison: SW implantation was modeled with SRIM [Stopping and Range of Ions in Matter, 11] for each element using the SW speed distribution from Genesis spacecraft measurements [12]. Measured and modeled profiles resemble each other quite well indicating good depth resolution of our technique (Figs. 2, 3). Deviations could be either due to some smearing of the former (knock-on of ions during analysis, ion channeling during implantation) or due to the fact that SRIM may not perfectly simulate the ion implant as, e.g., crystal structures are not accounted for. There is no evidence for diffusive loss of any of the analysed elements, including Na (Figs. 3e,f). The slow SW intensity peak, having the lowest implant energy, is closer to the surface and its ion distribution is more narrow (Figs. 2, 3a,b) than the fast SW. CME (Fig. 2) comprises a wide range of energies, including more energetic ions.

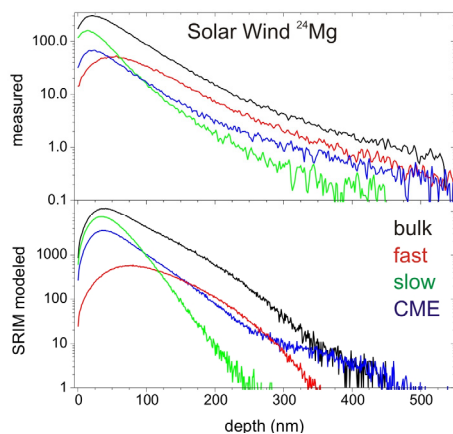


Fig. 2. Measured (sputter direction is from right) and modeled (SRIM, in Si) ^{24}Mg depth profiles in bulk and SW regimes (CME = coronal mass ejection). Y-axes are arbitrary, but the relative magnitude of the model data was normalized to the measured fluences.

Data reduction: Measured profiles were corrected for background and integrated. Final fluences were obtained from this integral extrapolated from the last measured point to the real target surface by using a quadratic polynomial (Figs. 3c-f). (At first, we tried to adjust repetitive SRIM curves, but none fit our measured Al, Ca, Na, Mg, and Cr profiles (see Figs. 3a,b).) The extrapolation should not introduce biases among SW regimes or relative elemental fluences.

Slow SW profiles and elements prone to contamination tend to require greater extrapolation. C,N,O SW profiles require the largest corrections as elevated amounts of O (natural oxide layer) and C, N (contamination, epoxy) were encountered soon after reaching the SW peak [6]. Two functions describe the measured data well: an asymmetric power function fits the entire profile, but, its extrapolation is asymptotic (Fig. 3c); thus, a quadratic polynomial calculated from peak to the front side was finally used to extrapolate to the real target surface. Accuracy of this approach can be seen for the case of Mg where the data go completely to the sample surface (Fig. 3 c,d). The excellent fit gives confidence to using this method for less complete profiles (that have at least 50% data coverage at the front side). SW fluences and implications are reported in [9].

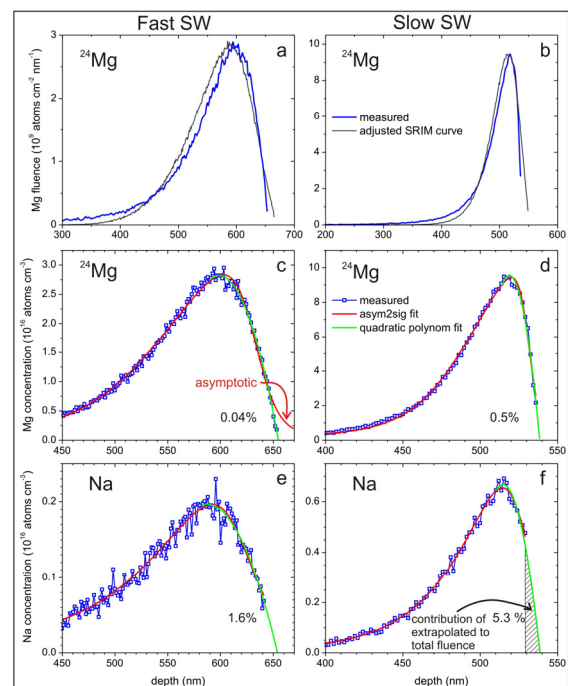


Fig. 3. Measured fast (a) and slow (b) ^{24}Mg SW profiles in comparison to their SRIM model curves (adjusted in height and position to measured data). (c)-(f) show ^{24}Mg and Na depth profiles measured in fast (c, e) and slow (d, f) SW and their respective fits used to extrapolate to the real target surface. Sputter direction is from left.

References: [1] Burnett, D.S., et al., (2003) *SSR* **105**: p. 509-534.[2] McKeegan, K.D., et al., (2011) *Science* **332**(6037): p. 1528-1532.[3] Heber, V.S., et al., (2012) *ApJ* **759**: p. 121-133.[4] von Steiger, R., et al., (2000) *J. Geophys. Res.* **105**(A12): p. 27217-27238.[5] Allton, J.H., et al. (2006) *37th LPSC*. #1611.[6] Heber, V.S., et al. (2010) *41st LPSC*. # 2234.[7] Huss, G.R., et al., (2012) *MAPS* **47**(9): p. 1436-1448.[8] Heber, V.S., et al. (2013) *44th LPSC*. # 3028.[9] Heber, V.S., et al. (2014) *45th LPSC*. [10] Burnett, D.S., et al., (2014 (in prep.)) *Geost. and Geoanal. Res.* [11] Ziegler, J.F., (2004) *Nucl. Instr. Meth. Phys. Res.* **219/220**: p. 1027-1036.[12] Reisenfeld, D.B., et al., (2013) *SSR*.